Journal of Nanotechnology and Materials Science

OMMEGA Publishers
Answering Intelligence

Research Article Open Access

Synthesis and Properties of (Co, Ni) Co-Doped ZnS Nanoparticles

B. Sreenivasulu, S. Venkatramana Reddy*, P. Venkateswara Reddy

Department of Physics, Sri Venkateswara University, Tirupati, Andhra Pradesh 517502, India

***Corresponding author**: S. Venkatramana Reddy, Department of Physics, Sri Venkateswara University, Tirupati, Andhra Pradesh 517502, India, E-mail: drsvreddy123@gmail.com

Abstract

Pure and (Co, Ni) co-doped ZnS nanoparticles are synthesized by using the chemical co-precipitation method. In this process Zinc Acetate [Zn $(CH_3COO)_2$. $2H_2O$], Sodium Sulfide (Na_2S), Nickel Chloride [$NiCl_2$.$6H_2O$] and Cobalt Acetate tetra hydrate [$Co(CH_3COO)_2$. $4H_2O$] act as precursor elements. Poly Vinyl Pyrrolidone (PVP) is used as capping agent. Pure ZnS and Cobalt doped at different concentrations (1, 3, 5 mol %) with Ni kept as constant at 3 mol % are grown. The X-ray diffraction (XRD) patterns indicate the formation of single phase cubic blended structure of pure and (Co, Ni) co-doped ZnS nanoparticles. From XRD calculations, the sizes of the pure and (Co, Ni) co-doped ZnS nanoparticles yield the range of 2 - 3 nm. The Raman peaks are observed at 263, 344 cm^{-1}, which are in good agreement with standard Raman transverse optical mode (TO) and longitudinal optical mode (LO), suggesting that the pure and co-doped samples have cubic blended structure. Optical absorption spectra show the absorption edge at 310 nm, in conformity with excitation and emission of PL spectra. The photoluminescence (PL) spectra exhibit the emission peaks in between 430 and 550 nm, which lie in UV and visible regions. SEM micro graphs show that the surface morphology of samples is nearly spherical; EDAX spectra depict the presence of Zn, S, Co and Ni in the chemical composition of samples in appropriate stoichiometric proportions. The micrographs recorded from Transmission Electron Microscope (TEM) show that the surface morphology of nanoparticles is spherical and average size of the nanoparticles is 15 nm. The magnetization measurements indicate the ferromagnetism in the synthesized samples at room temperature.

Received date: August 24, 2017
Accepted date: November 06, 2017
Published date: November 08, 2017

Citation: Reddy, S.V., et al. Synthesis and Properties of (Co, Ni) Co-Doped ZnS Nanoparticles J Nanotechnol Material Sci 4(3): 1- 7.

DOI: 10.15436/2377-1372.17.1657

Keywords: ZnS nanoparticles; XRD; Raman Studies; PL, Absorption spectra; SEM with EDAX; TEM and VSM.

Introduction

During the past years, the investigations for Diluted Magnetic Semiconductor (DMS) nanomaterials have attracted considerable attention due to their novel properties and broad application prospects in diverse areas, such as logic devices, spin polarized light emitting diode, spin field-effect transistors, field-emission devices, optical isolator, non-volatile memory devices and quantum computer, etc.[1-5] ZnS is a typical II-VI semiconductor material with direct wide band gap (3.67eV) and free exciting binding energy, and it is a versatile and multifunctional semiconductor material, in which a small fraction of host cations are replaced by transition metal (or) rare-earth ions which will effectively change the luminescence properties and magnetic properties of materials. In recent years, single transition metal doped ZnS have been extensively investigated by various methods. The crystal structure and band structure of ZnS can be modified by controlling the preparation process, changing the kinds of doping elements and doping amount, which further improve the magnetic and optical properties[6-10]. Many experimental results have recorded the room temperature ferromagnetism (RTFM) and extraordinary photoluminescence (PL) primarily depending on the synthesis method as well as processing conditions. Recently, some researchers investigated co-doped ZnS

nanocrystals to explore PL properties and RTFM enhanced by providing extra positive carriers in the host material[11-15]. But to the best of our knowledge, there is no report on the effect of the structural, optical and magnetic properties for (Co, Ni) co-doped ZnS nanomaterials.

In the present work, Pure ZnS and (Co, Ni) co-doped ZnS nanomaterials are synthesized by chemical co-precipitation method using Poly Vinyl Pyrrolidone (PVP) as stabilizer. The samples are characterized by X-ray diffraction (XRD), Scanning electron microscopy (SEM), high-resolution transmission electron microscopy (HRTEM), X-ray energy dispersive spectrometry (EDAX), Ultraviolet–visible spectroscopy (UV–visible), photoluminescence spectra (PL), Raman Spectra and the vibrating sample magnetometer (VSM) to investigate the crystal microstructure, morphology, constituent elements, optical and magnetic properties.

Sample preparation and experimental details

Pure and (Co, Ni) co-doped ZnS nanoparticles are synthesized by using simple chemical Co-precipitation method. The AR grade precursor materials such as Zinc Acetate [$Zn(CH_3COO)_2.2H_2O$], Sodium Sulfide (Na_2S), Nickel Chloride [$NiCl_2.6H_2O$] and Cobalt Acetate tetra hydrate [$Co(CH_3COO)_2.4H_2O$] are used in the sample preparation. To make $Zn_{1-(x+y)}Co_xNi_yS$ (x = 1, 3, 5 mol % and y = 3 mol %) composition, Zinc Acetate aqueous solution [$Zn(CH_3COO)_2.2H_2O$] is dissolved in de-ionized water and then Sodium sulfide aqueous solution is also added to the above solution drop-by-drop under constant magnetic stirring. After 2 min, white precipitate is formed. $NiCl_2.6H_2O$ and [$Co(CH_3COO)_2.4H_2O$] are added to the above precipitate under constant stirring and as a result (Co, Ni) co-doped ZnS nanoparticles are formed. To stabilize the nanoparticles, capping agent Poly Vinyl Pyrrolidone (PVP) is added to the solution. The precipitate is washed several times with de-ionized water and filtered out. The precipitate is dried at 80°C for 8 h for further characterization of the samples.

The prepared Samples are carefully subjected to the following characterization studies. Powder XRD pattern is recorded on Bruker diffractometer within the range of 20 – 80° using Cu Kα as X-ray source (λ = 1.53906 Å). The structure of pure and co-doped ZnS are analyzed by Raman Spectroscopy (LAB-RAM HR, HORIBA JOBIN–YVON Spectrophotometer). The optical properties are analyzed by UV–Vis diffusion reflectance Spectroscopy using CARY 5E UV–Vis-NIR Spectrophotometer in the wavelength range 200 – 2500 nm. The room temperature photoluminescence (PL) studies are carried out with EDINBURGH UV-VIS-NIR (FLS-980) spectrometer with Xenon arc lamp (450 W) as an excitation source. The surface morphology and chemical analysis of (Co, Ni) co-doped ZnS nanopowders are studied by SEM attached with Energy Dispersive Analysis of X- ray Spectra (EDAX) (model CARL—ZEISS EVOMA 15). Transmission electron microscopy (TEM) and selected area electron diffraction (SAED) are recorded on a Technai G20-Stwin High Resolution Transmission Electron Microscope (HR-TEM) using an accelerating voltage of 200 kV. Investigations of magnetic properties at the room temperature are carried out using a VSM magnetometer (Make and Model: Lakeshore, USA, Model 7407) at 17 X 10^3 gauss.

Results and discussions

XRD studies

X-ray diffraction pattern will give the information about grain size and crystalline structure of the nanoparticles. Figure 1 shows the XRD patterns of pure, and Co (1, 3, 5 mol %) and 3 mol% of Ni doped ZnS nanoparticles. It is clearly evident from XRD pattern that the diffraction peak (2θ) values are 28.88^0, 48.22^0 and 57.66^0.The peaks appear due to reflection from the (111), (220) and (311) planes, all the samples could be indexed to cubic structure of ZnS (JCPDS Card No. 80 - 0020). No diffraction peaks associated with any other impurities related to the dopants are observed in all the (Co, Ni) co-doped samples within the detection limit of the XRD. The peak positions of the co- doped samples lightly shift towards higher 2θ values, which clearly implies the smaller ionic radius of Co^{2+} (0.58 Å) compared to that of Zn^{2+} (0.74Å) in the ZnS The peak positions of Ni doped and Ni^{+} co- doped samples show a slight shift towards lower 2θ values, because the ionic radius of Ni (0.69 Å) is smaller than that of Zn. The above results indicate that the successful incorporation of Co^{2+} and Ni^{2+} ions in to the ZnS matrix and occupy the Zn^{2+} sites. On the other hand, it is observed that the replacement of Zn^{2+} ions by Co^{2+} and Ni^{2+} ions result in decrease in intensity of the XRD peaks, which implies that the degree of crystallinity of the samples decreases. Crystalline sizes are estimated from XRD analysis by using Scherer formula,

$$D = (0.91\ \lambda) / (\beta \cos\theta)$$

Where D is the average size of the particle, λ is the wavelength of the X-rays, β is the full width at half maximum intensity of the diffraction peak and θ is the diffraction angle. The average crystallite size of the particles is found to be in the range of 2 - 3 nm.

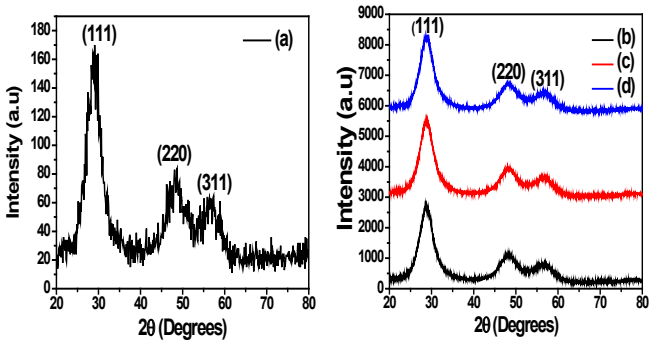

Figure 1: XRD Spectra of (a) Pure ZnS and (b) 1 mol % Co, (c) 3 mol % Co and (d) 5 mol % Co, co-doped with 3 mol % of Ni into ZnS nanoparticles.

Raman studies

Raman scattering is a very good tool to investigate the nanomaterials and presence of lattice defects in solids[16] within the material for further confirming, the formation of phase for all the synthesized samples. The Raman spectra of ZnS poly types have been described by Schneider and Kirby[17]. Nilsen et al.[18] have reported the one- and two-phonon Raman spectra of bulk cubic ZnS. For bulk cubic ZnS, the transverse optical (TO) and longitudinal optical (LO) zone center phonons have been observed at 270 and 350 cm^{-1} respectively. Room temperature Raman spectra of pure and (Co, Ni) co-doped ZnS nanoparticles recorded in the frequency range 200 - 450 cm^{-1} are shown in Figure 2. The peaks observed at 263 and 342 cm^{-1} may therefore

be assigned to TO and LO phonon modes respectively as reported by S. Kumar et al[19]. The observed broadening of the Raman peaks and their shifting towards lower energy as compared to the bulk values indicate quantum confinement effects in (Co, Ni) co-doped ZnS nanoparticles. As the carrier concentration in the semiconductor increases, the frequency of + L mode increases from bulk LO mode frequency and the frequency of - L mode increases from zero to TO mode frequency. Hence, the peak at 263 cm^{-1} observed in the present sample can be attributed to the TO mode. The Raman peak observed at 342 cm^{-1} can be assigned as the LO mode of co-doped cubic ZnS. The position of the TO mode is slightly different for 3 mol % of (Co, Ni) doped ZnS. This may be due to two reasons, first may be due to small amount of compressive strain and second may be due to large number of sulfur (S) vacancies. No other impurity peaks are observed, which support the effective doping of (Co, Ni) into ZnS under the presence of capping agent (PVP).

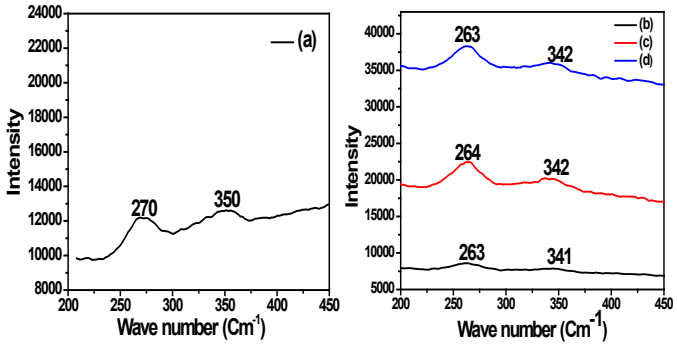

Figure 2: Raman Spectra of (a) Pure ZnS and (b) 1 mol % Co, (c) 3 mol % Co, (d) 5 mol % Co, co-doped with 3 mol % of Ni into ZnS nanoparticles.

Photoluminescence (PL) studies

The photoluminescence (PL) is one of the most important physical properties in ZnS nanoparticles and it depends upon synthesis conditions, shape, size and energetic position of the surface states[20-22]. The PL emission spectra of pure and (Co, Ni) co-doped ZnS nanoparticles are recorded at room temperature with excitation wave length 306 nm as shown in figure-3. The PL spectra show the sharp emission peaks for pure ZnS at 417 nm, 438 nm, and 466 nm are observed. The peak at 417 nm is lower than the band gap of the bulk ZnS (3.67 eV). The co-doped samples, Co (1,3, 5 mol %) with 3 mol % of Ni show the emission peaks at 436 nm, 449 nm, 467 nm, and 540 nm are observed, which are sharp with increased intensity.

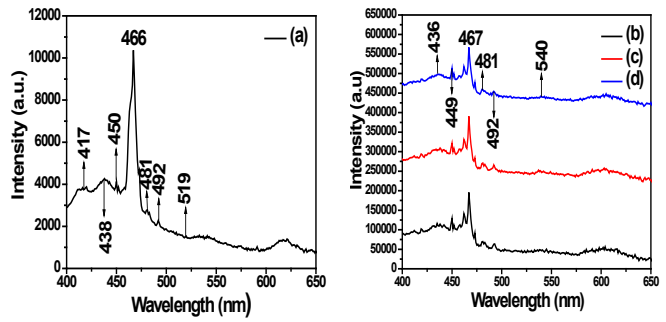

Figure 3: PL Spectra of (a) Pure ZnS and (b) 1 mol % Co, (c) 3 mol % Co, (d) 5 mol % Co, co-doped with 3 mol % of Ni into ZnS nanoparticles.

PL emission spectra of Pure and (Co, Ni) co-doped ZnS nanoparticles have sharp intensity and symmetric with four dominant peaks covering the whole UV visible region. The first three peaks at 436 nm, 449 nm, 467 nm corresponding to blue emission and the fourth peak at 540 nm is identified as green emission. This indicate that the involvement of different luminescent centers in the radiative process[23]. Different groups have studied the origin of blue luminescence from pure ZnS nanoparticles[24-28]. Sapara.et al reported PL emission at 466 nm from pure ZnS samples to de-excitation defect state upon 306 nm UV excitation. It is well known that the schottky defects are dominating in cubic ZnS[29]. The emission peak at 466 nm is attributed to sulfur vacancies. Borse.et al[30] and Lu.et al[31] have reported the peak observed in the range 450 - 460 nm is assigned to sulfur vacancies i.e., to the recombination of electrons at sulfur vacancy with holes in the valence band. The origin of emission peak observed at 467 nm does not result from impurity states related with co-dopant, but originated from native defect state. Similar PL peak has been observed around this wavelength range and attributed to emission from trap states in ZnS that are related to native zinc vacancy[32-33]. The green emission peak in the range 540 nm may be a result of recombination between the donar levels (S vacancy) and the levels of dopant ions that replaced Zn^{2+} ions in the ZnS host matrix[34-35]. In the ZnS samples co-doped with Cu^{2+} and Co^{2+}, it has been reported that the emission wavelength extended to lower energy that is around 515 – 560 nm. According to the present experimental results, Co^{2+} acts as sensitizing agent and shows the radiative recombination process and is enhanced in the lower concentration. Thus the fluorescence efficiencies at lower concentration are higher than those of higher concentrated (Co, Ni) co-doped ZnS samples.

UV–visible absorption spectra

The UV–visiable spectroscopy is a suitable method for investigating the impurity effects and co-doping on the optical properties of a ZnS nanoparticle, because co-doped ZnS nanoparticles have different optical properties in comparison with pure ZnS. The absorption spectra of pure and (Co, Ni) co-doped ZnS nanoparticles are shown in Figure. 4. The absorption shoulder peak at 320 nm is assigned to the characteristic absorption band edge of ZnS nanoparticles, which is blue, shifted as compared with the corresponding bulk band gap (3.67 eV) of ZnS due to quantum confinement effect[36]. However, the absorption edge for the (Co, Ni) co-doped ZnS nanoparticles is slightly shifted to shorter wavelengths (blue shift) compared to pure ZnS. The fundamental absorption, which corresponds to electron excitation from the valance band to conduction band, can be used to determine the value of the optical band gap of the synthesized (Co, Ni) co-doped ZnS nanoparticles. The relation between the incident photon energy (hυ) and the absorption coefficient (α) is presented by the following relation:

$$(\alpha h\upsilon)^{1/n} = A(h\upsilon - E_g)$$

Where A is the constant and E_g is the band gap energy of the material and n is the exponent that depends on the type of transition.

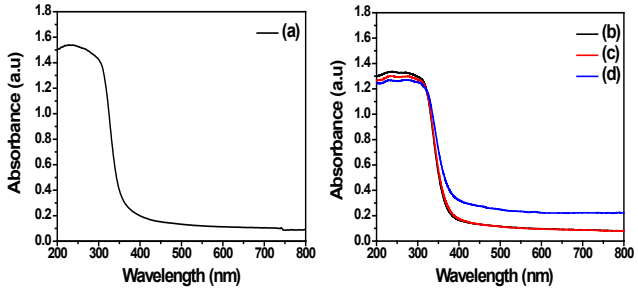

Figure 4: UV-Absorbtion Spectra of (a) Pure ZnS and (b) 1 mol % Co, (c) 3 mol % Co, (d) 5 mol % Co, co-doped with 3 mol % of Ni into ZnS nanoparticles.

SEM with EDAX

The surface morphology of Co (1, 3, 5 mol %) co-doped with 3 mol % of Ni into ZnS nanoparticles, is confirmed by EDAX spectra. Figure-5 shows the SEM images of co-doping of (Co, Ni) into ZnS nanoparticles, which are homogeneously distributed and their agglomeration has decreased with capping agent (PVP).

From SEM images, the obtained particles are nearly spherical in shape; this is confirmed by the TEM image of the samples. From the TEM micrograph, it is evident that the morphology of the (Co, Ni) co-doped sample seems to be nearly spherical in shape and the average particle size is in the order of 3 - 4 nm and is in good agreement with XRD results of (Co, Ni) co-doped ZnS nanoparticles.

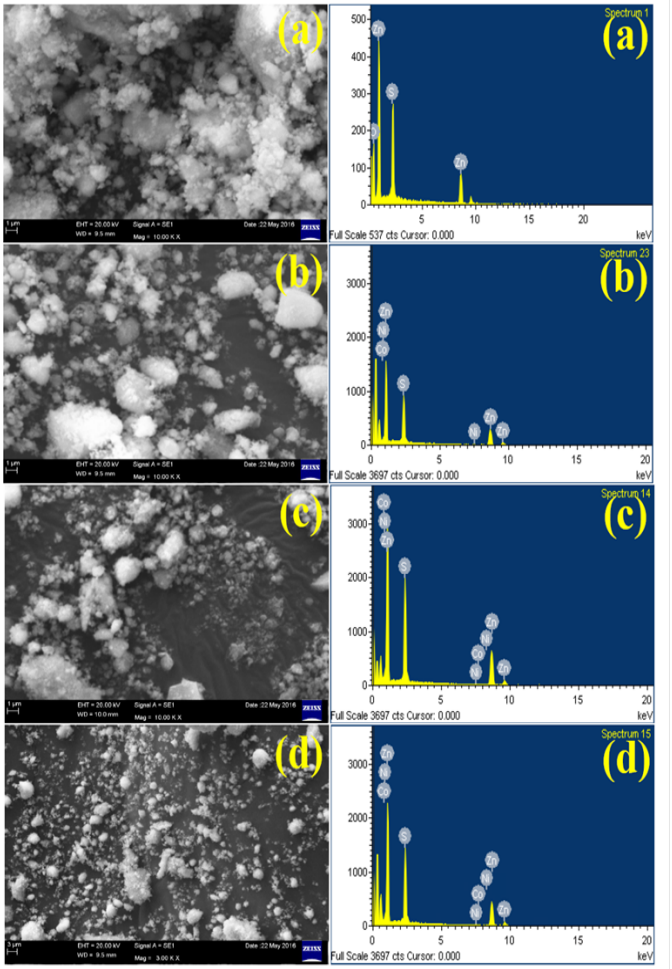

Figure 5: SEM with EDAX Micrographs of (a) Pure ZnS and (b) 1 mol % Co, (c) 3 mol % Co, (d) 5 mol % Co, co-doped with 3 mol % of Ni into ZnS nanoparticles.

Table 1: Chemical composition of pure and (Co, Ni) co-doped ZnS nanoparticles.

Element Sample	Zn		S		Co		Ni	
	Weight %	Atomic %	Wight %	Atomic %	Weight %	Atomic %	Weight %	Atomic %
Pure ZnS	58.28	20.19	41.72	79.81	0.00	0.00	0.00	0.00
1 mol % Co and 3 mol% Ni	68.46	51.72	31.13	47.94	0.21	0.17	0.20	0.17
3 mol % Co and 3 mol% Ni	68.09	51.25	31.62	48.51	0.05	0.04	0.24	0.20
5 mol % Co and 3 mol% Ni	67.27	50.37	32.26	49.24	0.12	0.10	0.35	0.29

TEM, HRTEM and SAED analysis

TEM is a good tool to investigate the structure and morphology of materials. TEM images of pure and (Co, Ni) co-doped ZnS nanoparticles are shown in Figure -6. TEM images show that the nanoparticles are nearly spherical in shape and quite uniform in morphology. The average particle size of pure and (Co, Ni) co-doped ZnS nanoparticles are found to be 5 nm, which is in good agreement with the average particle size obtained using XRD results. Both XRD and the TEM measurements suggest that most of the Co^{2+} and Ni^{2+} atoms have substituted into the ZnS lattice sites. The particles agglomeration decreases by adding Poly Vinyl Pyrrolidone (PVP) and stabilizes the crystallinity of nanoparticles. The high crystallinity of particles is confirmed by selected area electron diffraction (SAED) and high resolution (HR) TEM analysis as shown in Figure-6. The SAED pattern of pure and (Co, Ni) co-doped ZnS nanoparticles is consistent with cubic structure of ZnS corresponding to the strong ring pattern assigned to (111), (220) and (311) planes.

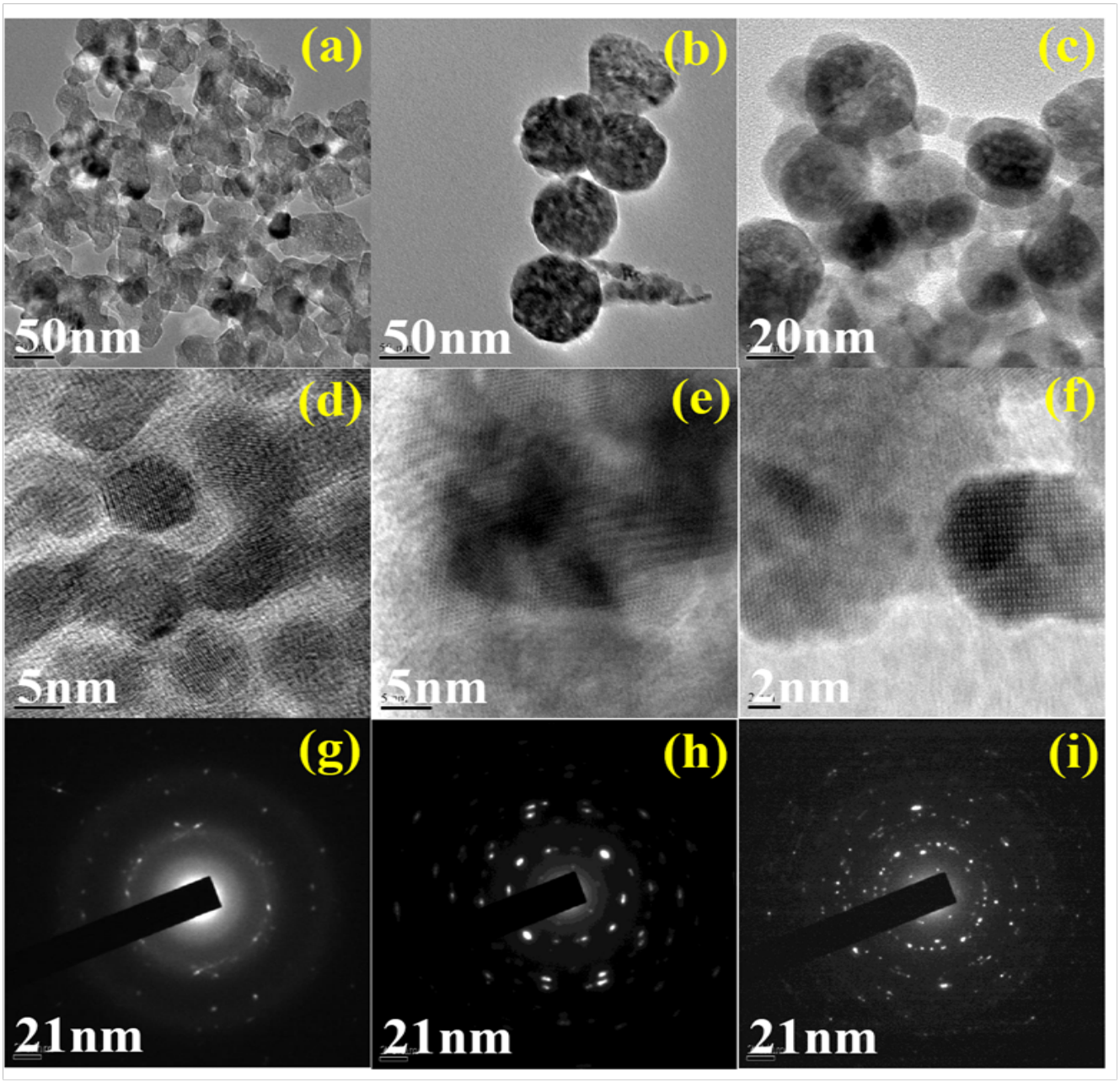

Figure 6: (a)–(c) TEM micro graphs, (d)–(f) HR -TEM micrographs and (g) - (i) SAED Micrographs of pure ZnS and $Zn_{1-(x+y)}$ Co_xNi_yS (x = 1, 3, 5 mol % and y = 3 mol %) nanoparticles.

VSM analysis (Magnetic Studies)

The magnetic properties of (Co, Ni) co-doped ZnS nanoparticles are measured by Vibrating Sample Magnetometer (VSM) at room temperature. The magnetic hysteresis loop of the $Zn_{1-(x+y)}$ Co_xNi_yS (x = 1, 3, 5 mol % and y = 3 mol %) nanoparticles can be seen clearly in Figure-7, which indicates the room temperature ferromagnetism of the prepared sample. But the pure ZnS shows the expected diamagnetic nature due to the absence of un paired electrons in its'd' orbital, which is not shown in figure.

The M–H curves indicate the saturation magnetization (M) values of 183.46 emu/g, 100.86 emu/g and 110.07 emu/g and Co-ercivity values of 742.72 G, 7106.54 G, and 576.93 G for $Zn_{1-(x+y)}$ Co_xNi_yS (x = 1 mol % and y = 3 mol %), $Zn_{1-(x+y)}$ Co_xNi_yS (x = 3 mol % and y = 3 mol %), and $Zn_{1-(x+y)}$ Co_xNi_yS (x = 5 mol % and y = 3 mol %) respectively. These values are mentioned in table.2. The saturation magnetization of (Co, Ni) co-doped sample is greater than that of pure ZnS, and the values of saturation magnetization increases (for 1 mol %) and slightly decreases (for 3, 5 mol %) with the increase of co- doping concentration. It is because that the Co^{2+} and Ni^{2+} ions substitute the Zn^{2+} ions, with the local hole concentration at the anion increasing. The local density of states at the Fermi level increases and exchange interaction is enhanced leading to enhance ferromagnetism. In view of the Co^{2+} and Ni^{2+} ions substituted into ZnS lattice, the origin of magnetism in the samples is due to the exchange interaction between local spin-polarized electrons (such as the electrons of Co^{2+} and Ni^{2+} ions) and the conductive electrons. Such interaction can lead to the spin polarization of conductive electrons. Consequently, the spin-polarized conductive electrons undergo an exchange interaction with local spin-polarized electrons of other Co^{2+} and Ni^{2+} ions. Thus, after a successive long-range exchange interaction, almost all Co^{2+} and Ni^{2+} ions exhibit the same spin direction, resulting in the

ferromagnetism of the material.

The present (Co, Ni) co-doped samples are prepared at 80°C. Thus tentatively the resulting ferromagnetic behavior of the present co-doped samples may be attributed to the substitution of Co^{2+} and Ni^{2+} in place of Zn^{2+} in ZnS host lattice without changing the structure which implies that this may be carrier induced ferromagnetism. Sambasivam et al.[37] also have reported such carrier induced ferromagnetism in Co doped ZnS nanoparticles, but they have reported a decrease in the magnetization with increasing Co concentration which they have attributed to anti ferromagnetic ordering with increasing Co concentration (10, 20 and 30 mol %). Perhaps they have used much higher Co concentrations in their samples, which lie outside the range of the present study. This might lead to strong anti ferromagnetic ordering and hence it is not proper to compare with the present trend. Recently Patel et al.[38] also have reported low temperature ferromagnetism in 2.5 at % Co and room temperature ferromagnetism in 5 at % cobalt doped ZnS thin films and suggested that the grain boundaries may play a role in bringing about the ferromagnetic order.

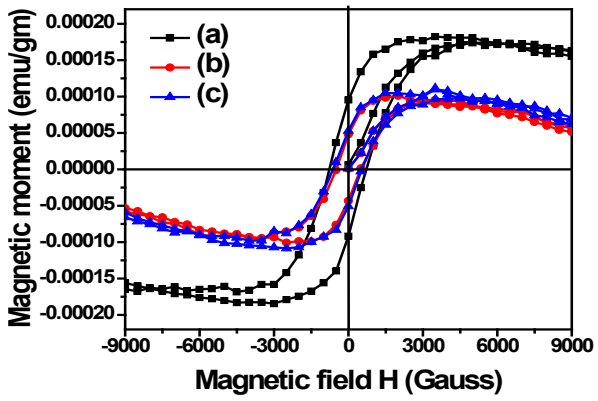

Figure 7: Room temperature M-H plots of (a) 1 mol % Co, (b) 3 mol % Co, (c) 5 mol % Co, co-doped with 3 mol % of Ni into ZnS nanoparticles.

Table 2: Magnetic Properties of (Co, Ni) co-doped ZnS nanoparticles.

Sample	Magnetization (emu)	Coercivity (G)	Retentivity (emu)
1% Co and 3% Ni	183.46 X 10^{-6}	742.72	93.497 X 10^{-6}
3% Co and 3% Ni	100.86 X 10^{-6}	7106.5	45.706 X 10^{-6}
5% Co and 3% Ni	110.07 X 10^{-6}	576.93	51.89 X 10^{-6}

Summary and conclusion

Pure and co-doped Co (1, 3, 5 mol %) with 3 mol% of Ni into ZnS nanoparticles are synthesized by chemical co-precipitation method. The XRD analyses show that the synthesized ZnS nanoparticles have Cubic blended structure. Raman spectra exhibit Raman peaks for pure and (Co, Ni) co-doped samples confirming the Cubic blended structure and shows quantum confinement in ZnS, which is in good agreement with XRD data. The surface morphology and chemical composition are examined using SEM with EDAX spectra. The absorption spectra of co-doped sample show absorption shoulder at 320 nm, which is blue shifted from bulk and the (Co, Ni) co-doped samples show absorption in the visible region without any sharp absorption peak in the absorption spectra. PL studies show strong UV emission at 467 nm and the intensity peaks covering the whole UV visible region. TEM micro graphs show that the surface morphology of pure ZnS and (Co, Ni) co-doped ZnS nanoparticles is spherical in shape and average diameter of nanoparticles is around 5 - 6 nm. VSM measurements show room temperature ferromagnetism in (Co, Ni) co-doped ZnS nanoparticles, and the saturation magnetization increases with the increase of co- doping concentration.

Acknowledgments: The authors wish to express their gratitude to Prof. Y. Prabhakara Reddy (Retd.), Department of Physics, S.V. University, Tirupati for his critical discussions during the course of Investigation.

References:

[1] Kimi, M., Yuliati, L., Shamsuddin, M. Preparation and characterization of in and Cu co-doped ZnS photocatalysts for hydrogen production under visible light irradiation. (2016) J Energy Chem 25(3): 512–516.
Pubmed | Crossref | Others

[2] Kumar, S., Verma, N.K. Effect of Ni-doping on optical and magnetic properties of solvothermally synthesized ZnS wurtzite nanorods. (2014) J Mater Sci Mater Electron 25(2): 785–790.
Pubmed | Crossref | Others

[3] Iqbal, M.J., Iqbal, S. Synthesis of stable and highly luminescent beryllium and magnesium doped ZnS quantum dots suitable for design of photonic and sensor material (2013) J Lumin 134: 739–746.
Pubmed | Crossref | Others

[4] Tang, J., Wang, K.L. Electrical spin injection and transport in semiconductor nanowires: challenges, progress and perspectives. (2015) Nanoscale 7(10): 4325–4337.
Pubmed | Crossref | Others

[5] Nasser, R., Elhouichet, H., Férid, M. Effect of Mn doping on structural, optical andphotocatalytic behaviors of hydrothermal Zn1−xMnxS nanocrystals. (2015) Appl Surf Sci 351: 1122–1130.
Pubmed | Crossref | Others

[6] Steger, M., Saeedi, K., Thewalt, M.L.W., et.al. Quantum Information Storage for over 180 s Using Donor Spins in a 28Si "Semiconductor Vacuum". (2012) Science 336: 1280–1283
Pubmed | Crossref | Others

[7] Liu, C., Meng, D., Pang, H., et al. Influence of Fe-doping onthe structural, optical and magnetic properties of ZnO nanoparticles. (2012) J Magn Magn Mater 324(20): 3356–3360.
Pubmed | Crossref | Others

[8] Sharma, D., Malik, B.P., Gaur, A. Two and four photon absorption and nonlinear refraction inundoped, chromium doped and copper doped ZnS quantum dots. (2015) J Phys Chem Solids 87: 163–170.
Pubmed | Crossref | Others

[9] Yin, Z., Zhang, J., Xu, K. Structural, electronic and optical properties of Zn0.5Cr0.5S from first-principles. (2016) Comput Mater Sci 112: 39–43.
Pubmed | Crossref | Others

[10] Goktas, A., Mutlu, I.H. Structural, Optical, and Magnetic Properties of Solution-Processed Co-Doped ZnS Thin Films. (2016) J Electron Mater 45(11): 5709–5720.
Pubmed | Crossref | Others

[11] Talwatkar, S.S., Sunatkari, A.L., Tamgadge, Y.S., et al. Influence of Li^{+} and Nd^{3+} co-doping on structural and optical properties of l-arginine-passivated ZnS nanoparticles. (2015) Appl Phys A 118 (2): 675–682.
Pubmed | Crossref | Others

[12] Kaur, P., Kumar, S., Singh, A., et al. Improved magnetism in Cr doped ZnS nanoparticles with nitrogen co-doping synthesized using chemical co-precipitation technique. (2015) J Mater Sci Mater Electron 26 (11): 9158–9163.
Pubmed | Crossref | Others

[13] Ashokkumar, M., Muthukumaran, S. Effect of Ni doping on electrical, photoluminescence and magnetic behavior of Cu doped ZnO nanoparticles. (2015) J Lumin 162: 97–103.
Pubmed | Crossref | Others
[14] Poornaprakash, B., Poojitha, P.T., Chalapathi, U., et al. Synthesis, structural, optical, and magnetic properties of Co doped, Sm doped and Co+Sm co-doped ZnS nanoparticles. (2016) Phys E Low-Dimens Syst Nanostructures 83: 180–185.
Pubmed | Crossref | Others
[15] Chen, H., Chen, C. Comparative studies on magnetic properties of Mn/Fe codoped ZnS nanowires. (2013) J Magn Magn Mater 330: 66–71.
Pubmed | Crossref | Others
[16] Torchynska, T.V., Hernandez, A.V. Cano, A.D., et al. Raman-scattering and structure investigations on porous SiCSiC layers. (2005) J Appl Phys 97(3)
Pubmed | Crossref | Others
[17] Schneider, J., Kirby, R.D. Raman Scattering from ZnS Polytypes. (1972) Phys Rev B 6 6(4): 1290–1294.
Pubmed | Crossref | Others
[18] Nilsen, W.G. Raman Spectrum of Cubic ZnS. (1969) Phys Rev 182: 838–850.
Pubmed | Crossref | Others
[19] Kumar, S., Chen, C.L., Dong, C.L., et al. Room temperature ferromagnetism in Ni doped ZnS nanoparticles. (2013) J Alloys Comp 554: 357–362
Pubmed | Crossref | Others
[20] Chen, W., Wang, Z.G., Lin, Z.J., et al. Absorption and luminescence of the surface states in ZnS nanoparticles. (1997) J Appl Phys 82: 3111
Pubmed | Crossref | Others
[21] Arai, T., Yoshida, T., Ogawa, T. Photoacoustic and Luminescence Spectra of CdS Fine Particles. (1987) J Appl Phys 26: 396
Pubmed | Crossref | Others
[22] Agata, M., Kurase, H., Hayashi, S., et al. Photoluminescence spectra of gas-evaporated CdS microcrystals. (1990) Solid State Commun 76 (8): 1061-1065
Pubmed | Crossref | Others
[23] Sarkar, R., Tiwary, C.S., Kumbhakar, P., et al. Yellow-orange light emission from Mn^{2+}-doped ZnS nanoparticles. (2008) Physica E 40 (10): 3115- 3120
Pubmed | Crossref | Others
[24] Manzoor, K., Vadera, S.R., Kumar, N., et al. Synthesis and photoluminescent properties of ZnS nanocrystals doped with copper and halogen. (2003) Mater Chem Phys 82 (3):718-725
Pubmed | Crossref | Others
[25] Sooklal, K., Cullum, B., Michael, S., et al. Photophysical Properties of ZnS Nanoclusters with Spatially Localized Mn^{2+}. (1996) J Phys Chem 100 (11): 4551-4555
Pubmed | Crossref | Others
[26] Karar, N., Singh, F., Mehta, B.R. Structure and photoluminescence studies on ZnS:Mn nanoparticles. (2004) J Appl Phys 95 (2): 656-660.
Pubmed | Crossref | Others
[27] Sapara, S., Prakash, A., Ghangrekar, A., et al. Emission Properties of Manganese-Doped ZnS Nanocrystals. (2005) J Phys Chem B 109:1663- 1670.
Pubmed | Crossref | Others
[28] Chen, W., Aguekian, V.F., Vassiliev, N., et al. New observations on the luminescence decay lifetime of Mn^{2+} in ZnS: Mn^{2+} nanoparticles. (2005) J Chem Phys 123 (12): 124707
Pubmed | Crossref | Others
[29] Kumar, S.S., Khadar, M.A., Dhara, S.K., et al. Photoluminescence and Raman studies of ZnS nanoparticles implanted with Cu^{+} ions. (2004) Nucl Intrum Meth B 251(2): 435–440.
Pubmed | Crossref | Others
[30] Borse, P.H., Deshmukh, N., Shinde, R.F., et al. Luminescence quenching in ZnS nanoparticles due to Fe and Ni doping. (1999) J Mater Sci 34 (24): 6087–6093.
Pubmed | Crossref | Others
[31] Lu, H.Y., Chu, S.Y., Tan, S.S. The characteristics of low-temperature-synthesized ZnS and ZnO nanoparticles. (2004) J Cryst Growth 269 (21-4): 385–391.
Pubmed | Crossref | Others
[32] Joo, J., Na, H.B., Yu, T., et al. Generalized and Facile Synthesis of Semiconducting Metal Sulfide Nanocrystals. (2003) J Am Chem Soc 125 (36): 11100–11105.
Pubmed | Crossref | Others
[33] Karar, N., Singh, F., Mehta, B.R. Structure and photoluminescence studies on ZnS:Mn nanoparticles. (2004) J Appl Phys 95 (2):656–660.
Pubmed | Crossref | Others
[34] Xu, S.J., Chua, S.J., Liu, B., et al. Luminescence characteristics of impurities-activated ZnS nanocrystals prepared in microemulsion with hydrothermal treatment. (1998) Appl Phys Lett 73 (4): 478–480.
Pubmed | Crossref | Others
[35] Peng, W.Q., Cong, G.W., Qu, S.C., et al. Synthesis and photoluminescence of ZnS:Cu nanoparticles. (2006) Opt Mater 29(2-3): 313–317
Pubmed | Crossref | Others
[36] Rossetti, R., Hull, R., Gibson, J.M., et al. Excited electronic states and optical spectra of ZnS and CdS crystallites in the ≈15 to 50 Å size range: Evolution from molecular to bulk semiconducting properties. (1985) J Chem Phys 82: 552–559.
Pubmed | Crossref | Others
[37] Sambasivam, S., Paul Joseph, D., Lin, J.G., et al. Doping induced magnetism in Co–ZnS nanoparticles. (2009) J Solid State Chem 182 (10): 2598–2601.
Pubmed | Crossref | Others
[38] Patel, S.P., Pivin, J.C., Chawla, A.K., et al. Room temperature ferromagnetism in $Zn_{1-x}Co_xS$ thin films with wurtzite structure Mater. (2011) J Magn Magn 323: 2734-2740
Pubmed | Crossref | Others